25

Estimation of the Sea Level Rise by 2100 Resulting from Changes in the Surface Mass Balance of the Greenland Ice Sheet

Xavier Fettweis, Alexandre Belleflamme, Michel Erpicum,
Bruno Franco and Samuel Nicolay
University of Liège
Belgium

1. Introduction

The Surface Mass Balance (SMB) can be seen, in first approximation, as the water mass gained by the winter snowfall accumulation minus the mass lost by the meltwater run-off in summer. The mass gain from rainfall as well as the mass loss from erosion from the net water fluxes (the sum of the evaporation, sublimation, deposition and condensation) and from the wind (blowing snow) are negligible in the SMB equation of the Greenland Ice Sheet (GrIS) compared to the snowfall and the melt (Box et al., 2004). The ice sheet mass balance takes also into account the mass loss from iceberg calving. Consequences of a warmer climate on the Greenland ice sheet SMB will be a thickening inland, due to increased solid precipitation, and a thinning at the Greenland ice sheet periphery, due to an increasing surface melt. A climatic warming increases the snow and ice melting in summer but it enhances also evaporation above the ocean. This leads to higher moisture transport inland and, consequently, higher precipitation. The response of the iceberg calving to the climate change could be an acceleration of the glacier flow (Nick et al., 2009; Zwally et al., 2002) but these projections are very uncertain (Sundal et al., 2011) and a lot of developments are still needed in the glaciology models for improving our knowledge and modelling of the Greenland ice sheet dynamics. That is why we will focus our study only on the SMB of the Greenland ice sheet.

The IPCC (Intergovernmental Panel on Climate Change) projects, in response to global warming induced by human activities, that the run-off increase will exceed the precipitation increase and therefore that the currently observed surface melting of the Greenland ice sheet (Fettweis et al., 2011b; Tedesco et al., 2011; Van den Broeke et al., 2009) will continue and intensify during the next decades (IPCC, 2007). An increasing freshwater flux from the Greenland ice sheet melting could perturb the thermohaline circulation (by reducing the density contrast driving this last one) in the North Atlantic including the drift which tempers the European climate. In addition, an enduring Greenland ice sheet melting, combined with the thermal expansion of the oceans and the melt of continental glaciers, will raise the sea level with well-known consequences for countries such as the Netherlands, Bangladesh,... The contribution of the Greenland ice sheet SMB decrease to the sea level rise is currently evaluated to be 5-10 cm by 2100 (Gregory and Huybrechts, 2006; Fettweis et al.,

2008; Franco et al., 2011; IPCC, 2007; Mernild et al., 2010). However, despite their importance for the global climate, large uncertainties remain in these estimations because most of the current studies are based mainly on outputs from atmosphere–ocean general circulation models (called hereafter global models) not well suited to the polar regions and with a typical horizontal resolution of 300 km while the width of the ablation zone is lower than 100km.
In response to these uncertainties, the regional modelling is the ideal tool to provide some more precise answers to understand and quantify how the Greenland ice sheet SMB will respond to climate change. In particular, the regional climate model MAR (for *Modèle Atmosphérique Régional*) fully coupled with a snow model and extensively validated to simulate the SMB of the Greenland ice sheet (Fettweis et al., 2005; Fettweis, 2007; Fettweis et al., 2011b; Lefebre et al., 2003; 2005), is designated to study the Greenland climate at high resolution (25 km), with a physic developed for and well adapted to polar regions. Until now, the only future projections at high-resolution of the Greenland ice sheet SMB have been carried out with models not taking into account the atmosphere-snow feedbacks occurring above the melt area as the well known surface albedo positive feedback (Mernild et al., 2008; 2010). Therefore, we propose here to carry out future projections of Greenland climate with the MAR model coupled with a snow model and forced by two scenarios of greenhouse gas emissions made for the next IPCC assessment report (AR5). This work fits in the ICE2SEA project (http://www.ice2sea.eu) of the 7th Framework Program (FP7) which aims to improve the projections of the continental ice melting contribution to sea level rise.
After a brief description in Sect. 2 of the regional model we used, Sect. 3 evaluates, by comparison with the reanalysis and other IPCC AR5 global models (see Table 1), the global model CanESM2 which is used for forcing the MAR future projections. Sect. 4 validates the CanESM2-forced MAR simulation over the current climate (1970–1999) in respect to the ERA-40 forced MAR simulation. Future SMB projections of CanESM2-forced MAR simulations are analysed in Sect. 5. Finally, future projections of sea level rise coming from the Greenland ice sheet SMB decrease are given in Sect. 6.

2. Data

The model used here is the regional climate model MAR coupled to the 1-D Surface Vegetation Atmosphere Transfer scheme SISVAT (Soil Ice Snow Vegetation Atmosphere Transfer) (Gallée and Schayes, 1994). The snow-ice part of SISVAT, based on the CEN (*Centre d'Etudes de la Neige*) snow model called CROCUS (Brun et al., 1992), is a one-dimensional multi-layered energy balance model that determines the exchanges between the sea ice, the ice sheet surface, the snow-covered tundra, and the atmosphere. It consists of a thermodynamic module, a water balance module taking into account the meltwater refreezing, a turbulence module, a snow metamorphism module, a snow/ice discretization module, and an integrated surface albedo module (Gallée et al., 2001). The blowing snow model, currently under development, is not yet used here. SISVAT does not contain an ice dynamics module. Therefore, a fixed ice sheet mask (i.e. a fixed land surface classification of the pixels representing the Greenland ice sheet) and topography are assumed for simulating both current and future climates. This explains why we only present here the SMB and not the ice sheet mass balance of the Greenland ice sheet.
The MAR version used here is the one from Fettweis et al. (2011b) calibrated to best compare with the satellite derived melt extent over 1979-2009. Compared to the set-up of Fettweis et al. (2005; 2011b), a new tundra/ice mask is used here based on the Greenland land surface

classification mask from Jason Box (http://bprc.osu.edu/wiki/Jason_Box_Datasets) and the filtering of the Bamber et al. (2001) based topography is reduced by a factor two. The integration domain (shown in green in Fig. 1) as well as the spatial resolution (25 km) are the same than in Fettweis et al. (2005).
For studying the current climate, the ERA-40 reanalysis (1958–1999) and after that the ERA-INTERIM reanalysis (2000–2010) from the European Centre for Medium Range Weather Forecasts (ECMWF) are used to initialize the meteorological fields at the beginning of the MAR simulation in September 1957 and to force every 6 hours the MAR lateral boundaries with temperature, specific humidity and wind components during the simulation. The Sea Surface Temperature and the sea-ice cover are also prescribed by the reanalysis. No corrections are applied to the MAR outputs.

Model ID	Institutes, Country
BCC-CSM1-1	Beijing Climate Center, China
CanESM2	Canadian Centre for Climate Modelling and Analysis, Canada
CNRM-CM5	Centre National de Recherches Météorologiques et Centre Europeen de Recherche et Formation Avancées en Calcul Scientifique, France
GISS-E2	NASA Goddard Institute for Space Studies, USA
HadGEM2-ES	Met Office Hadley Centre, UK
INMCM4	Institute for Numerical Mathematics, Russia
IPSL-CM5A-LR	Institut Pierre Simon Laplace, France

Table 1. List of the seven IPCC AR5 global models available in June 2011 and used in this paper. These outputs are provided by the World Climate Research Programme's (WCRP's) Coupled Model Intercomparison Project phase 5 (CMIP5) multi-model dataset (http://cmip-pcmdi.llnl.gov/cmip5).

For computing future projections, we use the 6 hourly outputs of CanESM2 (see Table 2). The daily sea surface temperature and sea ice cover from CanESM2 are used to force the ocean surface conditions in SISVAT. The CanESM2-forced MAR simulation starts in September 1964 and lasts till December 2005 with the outputs from the Historical experiment (representing the current climate). The MAR future projections (2006-2100) use the CanESM2 outputs from two new scenarios (called RCP for Representative Concentration Pathways) of greenhouse gases concentration that will be used in the next IPCC report:

- **RCP 4.5**: mid-range scenario corresponding to a radiative forcing of $+4.5$ w/m^2 at stabilization in 2100. This scenario corresponds to an increase of the atmospheric greenhouse gas concentration during the 21st century to a level of 850 CO_2 equivalent p.p.m. by 2100.
- **RCP 8.5**: pessimistic scenario corresponding to a radiative forcing of $> +8.5$ w/m^2 in 2100. This scenario corresponds to an increase of the atmospheric greenhouse gas concentration during the 21st century to a level of $>$ 1370 CO_2 equivalent p.p.m. by 2100.

We refer to Moss et al. (2010) for more details about the RCP scenarios.

3. Comparison of CanESM2 with other IPCC AR5 models

The aim of this section is to gauge the ability of the IPCC AR5 global models to reproduce the present-day climate conditions over Greenland. A good representation of the current climate is a necessary, but not sufficient condition for the global model ability to simulate

MAR Forcing	Periode
ERA-40 reanalysis	1957-1999
ERA-INTERIM reanalysis	2000-2010
Historical experiment from CanESM2	1964-2005
RCP 4.5 experiment from CanESM2	2006-2100
RCP 8.5 experiment from CanESM2	2064-2100

Table 2. Summary of the different forcings used in the MAR simulations.

future climate change. Indeed, a model that fails to reproduce the current climate generates projections that lack in reliability and validity.
We will show that CanESM2 used for forcing MAR is one of the most suitable global models currently available from the CMIP5 data base for simulating the current climate (1970–1999) over Greenland in respect to the ERA-40 reanalysis. In addition, its future projections of temperatures are in the range of the other IPCC AR5 global models.

3.1 Evaluation over current climate

The global models listed in Table 1 from the CMIP5 data base are evaluated with the aim to use them as forcing of a regional model. The general atmospheric circulation in the regional model is fully induced by the global model-based boundaries forcing while the surface conditions (except the sea surface temperature and sea ice cover which are used as forcing) simulated by the global model do not impact the results of the regional model. This means that the regional model is not able to correct biases in the general circulation coming from the global models. In addition, Fettweis et al. (2011a) showed that the general circulation at 500hPa (gauged by the geopotentiel height) correlates significantly with the surface melt anomalies. Therefore, only the average state of the free atmosphere (here at 500hPa) is evaluated here.
As validation, the global model outputs at 500hPa coming from the Historical experiment (representing the current climate) are compared to the ERA-40 reanalysis over 1970–1999 (considered here as the reference period). Franco et al. (2011) showed that at 500hPa, both ERA-40 and NCEP-NCAR (National Centers for Environmental Prediction–National Center for Atmospheric Research) reanalyses compare very well and so a comparison with only the ERA-40 reanalysis is enough here. The fields which are evaluated are:

- **the mean temperature over the melt season** (from May to September and called summer hereafter). A global model-based temperature bias is propagated through the regional model boundaries inducing a similar temperature bias in the regional model which impacts the amount of simulated surface melt. Only CanESM2 satisfactorily simulates the mean summer temperature although it is too cold in the South and too warm in the North (see Fig. 1). HadGEM2-ES and INMCM4 are 2°C too warm at the north of the GrIS and the other global models are rather several degrees too cold in summer. The observed doubling of the amount of surface melt since 30 years corresponds to a warming of 2-3 °C (Fettweis, 2007; Fettweis et al., 2011a;b). Thus, it suggests that a bias in summer of several degrees at the regional model boundaries is not acceptable.
- **the mean temperature over the accumulation season** (from October to April and called winter hereafter). The global model-based temperature at the regional model boundaries impacts the maximum moisture content of the air masses and so it impacts the amount of precipitation simulated by the regional model. Except INMCM4, the global models are too cold in winter. The highest biases are observed for most of the models in the South-East of Greenland.

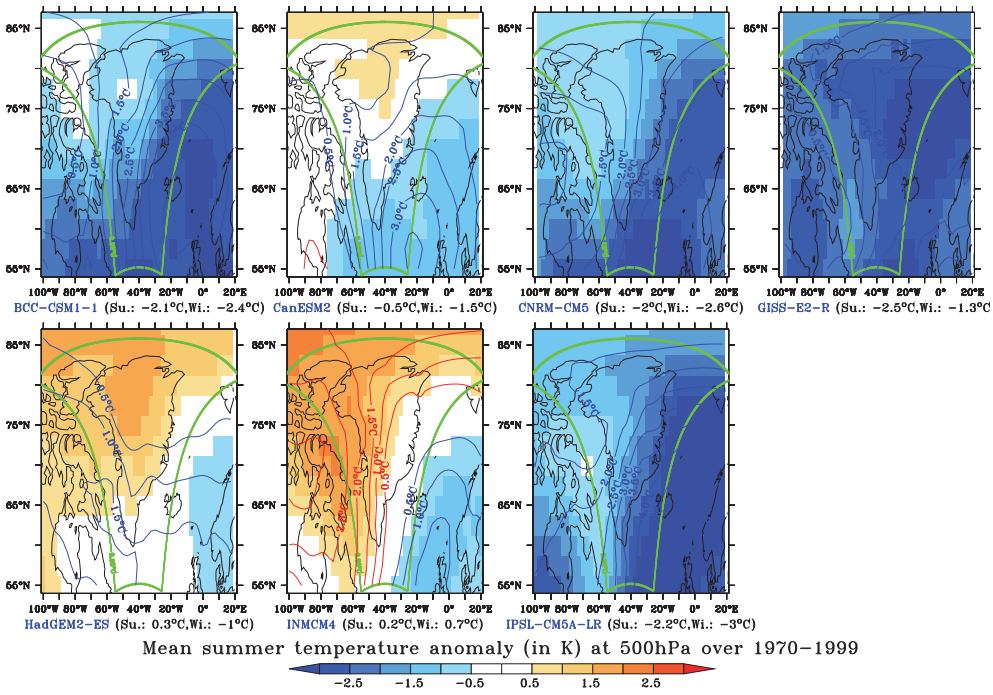

Fig. 1. Difference between the summer (May-Sep) mean 500 hPa temperature simulated by the global models for the Historical experiment and from the ERA-40 reanalysis over 1970–1999 (reference period). The solid lines in red (positive bias) and in blue (negative bias) plot the winter (Oct-Apr) mean 500 hPa temperature difference with regard to the ERA-40 reanalysis over 1970–1999. Units are degrees. The mean bias for winter (Wi.) and summer (Su.) is given in brackets. Biases above 1°C in Summer and 2°C in winter are statistically significant i.e. two times higher than the ERA-40 temperature standard deviation. Finally, the boundaries of the MAR integration domain are shown in green.

- **the annual mean wind speed**. Most of humidity comes into the regional model domain from the southern boundary situated in the storm tracks associated to the Icelandic Low. The wind speed at the regional model boundaries impacts the moisture advection into the integration domain and so the precipitation simulated by the regional model. The wind speed simulated by HadGEM2-ES compares the best with the reanalysis (see Fig. 2). CanESM2 overestimates the wind speed in the south of the domain while the other global models rather underestimate it.
- **the annual geopotential height**. This last one reflects the main general circulation pattern i.e. an eastward general circulation from the North American continent, adopting a north-west direction over Baffin Bay before reaching the western coast of Greenland, and generating a north-eastward circulation over central Greenland. In southern Greenland, the regional circulation is more influenced by meridional fluxes. Biases at the regional model boundaries in the direction of the main flows impact the precipitation pattern. Only GISS-E2-R does not clearly show an atmospheric circulation pattern which is consistent with the reanalysis. In addition, along the East Greenland coast, BCC-CSM1-1,

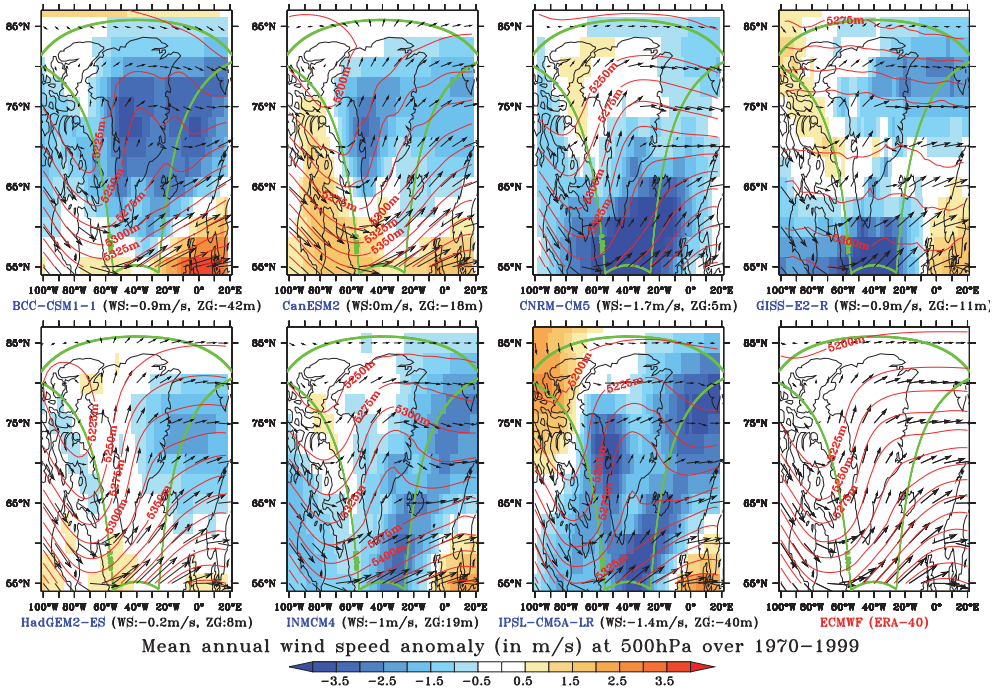

Fig. 2. Difference between the annual mean 500 hPa wind speed (in m/s) simulated by the global models for the Historical experiment and from the ERA-40 reanalysis over 1970–1999. The solid lines in red and arrows in black plot respectively the yearly mean 500 hPa geopotential height in meters and the wind vectors. Finally, as last plot, the mean 500 hPa geopotential height from the ERA-40 reanalysis is given as reference as well as the wind vectors. The mean bias of wind speed (WS) in m/s and geopotential height (ZG) in m are given in brackets.

INMCM4 and IPSL-CM5A-LR simulate a north-west component of the general circulation in disagreement with the reanalysis.

HadGEM2-ES (resp. CanESM2) is the top-performing model in simulating the present-day wind speed and circulation (resp. the summer temperature) at 500hPa. INMCM4 is too warm and the other global models are too cold and underestimate the wind speed. Knowing the importance of the global model summer temperature biases in the amount of the melt simulated by the regional model, CanESM2 has been selected as the most suitable candidate for forcing the MAR model. However, simulations of MAR forced by HadGEM2-ES should be performed in future because the general circulation and the winter temperatures simulated by HadGEM2-ES are better than the one simulated by CanESM2. However, HadGEM2-ES is too warm in summer. The main biases of CanESM2 are a wind speed overestimation (resp. underestimation) in the south (resp. north-west) of Greenland and a cold bias in winter.

3.2 Future projections

In Fig. 3, we see first that the run of CanESM2 used for forcing MAR captures well the temperature variability coming for the NCEP-NCAR reanalysis with a sharp increase of

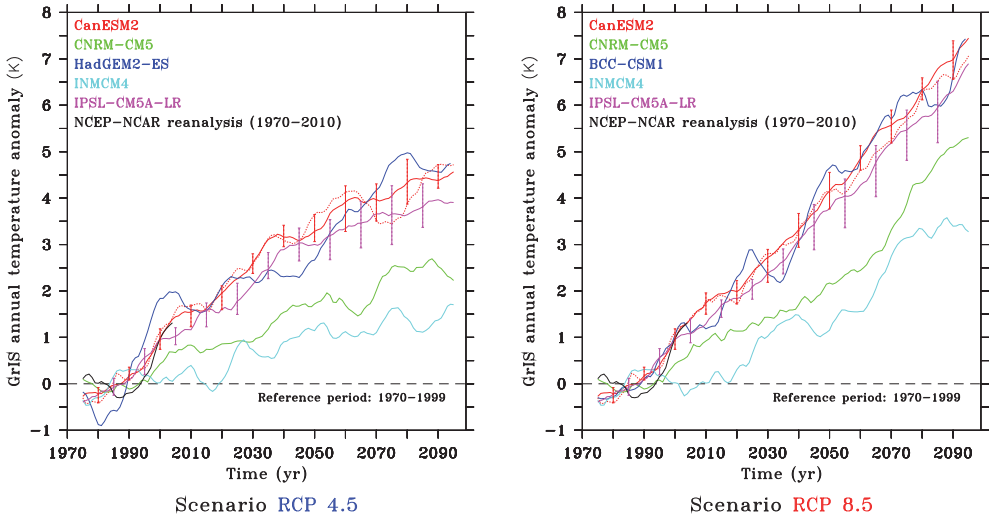

Fig. 3. Time series of the current and future projections of the Greenland ice sheet annual temperature anomalies (in respect to the 1970–1999 period) simulated by the global models for the RCP 4.5 (left) and RCP 8.5 (right) scenario and by the NCEP-NCAR reanalysis (representing the observed temperature variability of the last 40 years). A 10-year running mean is applied here and the Greenland ice sheet temperature variability is taken over an area covering Greenland: 60° W≤longitude≤20° W and 60° N≤latitude≤88° N. When several runs are available for a model (CanESM2 and IPSL-CM5A-LR), the average over all runs is shown and the error bar gives the range around this average. Finally, the run (called *r1i1p1*) of CanESM2 used for forcing MAR is shown in dotted red.

the temperature in the end of 1990's in respect to the 1970–1999 period. HadGEM2-ES simulates this temperature increase too early in the 1990's while INMCM4 and CNRM-CM5 underestimate it. About the future projections, we see that the CanESM2 future projections compare well with those ones from BCC-CSM1-1, HadGEM2-ES and IPSL-CM5A-LR while INMCM4 and CNRM-CM5 seem to be less sensitive over Greenland to the greenhouse gas concentration increase. At the end of the century, most of the global models project an annual temperature increase in the Greenland area of 4-5°C (resp. 7-8°C) for the RCP 4.5 (resp. RCP 8.5) scenario.

4. SMB evaluation of the CanESM2 forced MAR over current climate

As for the global models, it is important to evaluate, over the present-day climate, the regional model forced by the most suitable global model selected in the previous section. Before discussing future projections, we have first to check if MAR forced by the Historical experiment from CanESM2 is able to simulate the current surface conditions over the Greenland ice sheet. That is why, the CanESM2 forced MAR simulation is compared here over 1970–1999 with the ERA-40 forced MAR simulation considered as the reference simulation for the currently observed SMB over the Greenland ice sheet (Fettweis et al., 2011b).

4.1 Average annual rates of the SMB components

At the scale of the whole Greenland ice sheet, MAR forced by CanESM2 over 1970–1999 underestimates a few the SMB in respect to the ERA-40 forced run due to an underestimation of the winter accumulation (Oct-Apr) and an overestimation of the run-off (See Table 3). However, these biases are not significant and are included in the natural variability. Finally, the solid and liquid precipitation in Summer (May-Sep) as well as the net water fluxes compare well.

MAR forced by	SMB	Winter (WSF) Snowfall	Summer (SSF) Snowfall	Rainfall (RF)	Run-off (RU)	Meltwater (ME)	Net water fluxes (SU)
ERA-40	460±106	387±46	288±34	27±5	237±61	419±84	6±1
CanESM2	392±102	335±31	2891±42	36±8	263±78	421±107	5±2

Table 3. Average and standard deviation of the annual surface mass balance components simulated by MAR forced by ERA-40 and by CanESM2 over 1970–1999. Units are Gt/yr. The surface mass balance (SMB) equation is here SMB = WSF + SSF + RF - RU - SU. The run-off is the part of not refrozen water from both surface melt and rainfall reaching the ocean. Finally, the blowing snow sublimation is not taken into account in our simulation.

4.2 Temporal variability and trend of the SMB components

In average over 1970–1999, the CanESM2 forced MAR is significantly too cold in winter in respect to the ERA-40 forced run (Fig. 4) while the annual cycle of the mean Greenland ice sheet temperature is well reproduced. In summer, MAR simulations using both forcings compare well. This is in full agreement with the CanESM2 temperature biases versus ERA-40 shown in Fig 1.

The mean seasonal cycle of the melt area simulated by MAR forced by ERA-40 and CanESM2 compare very well knowing that the ERA-40 forced MAR simulation compare well with the microwave satellite derived one according to Fettweis et al. (2011b). However, although this is not significant, there is a delay of about 5 days between the CanESM2 and the ERA-40 forced simulations. The annual cycle of the bare ice area (i.e. the ablation zone where most of the melt takes place due to the lower albedo of bare ice compared to melting snow (Tedesco et al., 2011)) is also shown in Fig. 4. There is a significant overestimation through the whole melting season of the bare ice area if MAR is forced by CanESM2. This bias, due to an underestimation of the winter accumulation listed in Table 3, is explained in the next section.

Despite of the SMB components biases quoted in Section 4.1, the CanESM2 forced run reproduces very well the ERA-40 forced SMB components trends i.e. a decreasing of the SMB since the beginning of the 2000's associated to a quasi constant snowfall variability over 1970-2005 and an increasing trend of the run-off in agreement with the summer temperature changes (see Fig. 5).

4.3 Spatial variability

The CanESM2 forced SMB simulated by MAR is significantly too low in the north-west of the Greenland ice sheet and too high in the south and along the north-eastern coast (see Fig. 6).

The negative anomalies in the north-west are a conjunction of negative anomalies in snowfall and positive anomalies in run-off induced by biases in summer temperature and winter accumulation. In addition to impact directly the gained mass, a too low winter accumulation decreases the snowpack height above bare ice in the ablation zone which induces premature

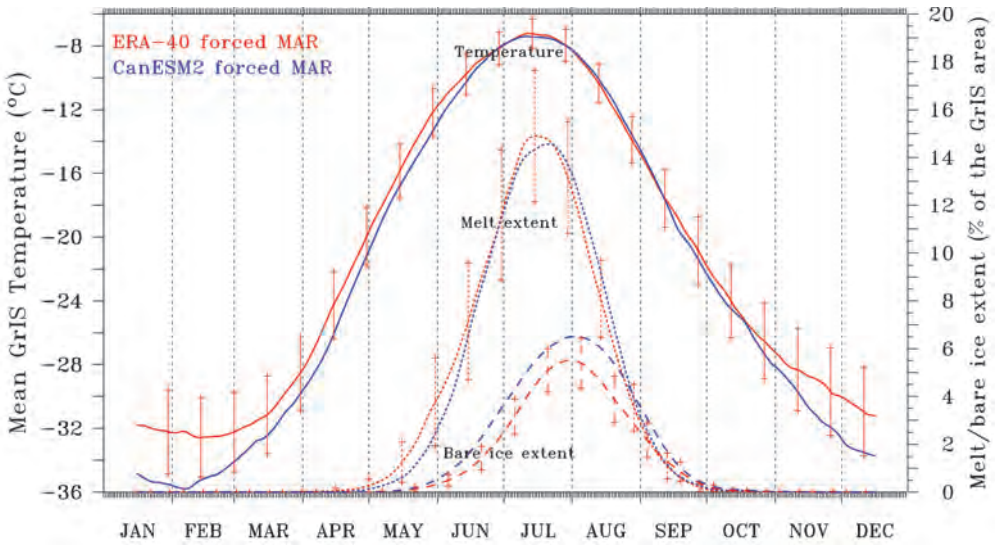

Fig. 4. Average over 1970–1999 of the mean Greenland ice sheet temperature annual cycle (left Y-axis) as well as the melt and bare ice extent simulated by MAR forced by ERA-40 (in red) and by CanESM2 (in blue) (right Y-axis). The melt extent is defined as the area where the daily meltwater production is higher than 8 mmWE according to Fettweis et al. (2011b) and the bare ice extent is the area where the surface snow density is higher than 900 kg/m^3. Finally, a 30 days running mean is applied here and the error bars plot the standard deviation over 1970–1999 around the ERA-40 forced mean.

bare ice exposure in summer, reducing the surface albedo and then enhancing the surface melt. This snowfall negative anomaly is due to an underestimation by CanESM2 of the south-westerly flow, common in this area (see Fig. 2), impacting the amount of moisture which is advected by MAR on this area. In the south of the ice sheet, in contrary, the westerly flow is overestimated by CanESM2 enhancing the precipitation in MAR. It should be remembered that biases at 500hPa in the large scale forcing are not corrected by the regional model even in the interior of its integration domain.

In addition to the winter accumulation induced biases, the run-off anomalies reflect the summer temperature biases i.e. MAR forced by CanESM2 is too cold in summer along the eastern and southern coasts and too warm along the western and northern coasts. Similar patterns of temperature biases are present in CanESM2 itself as shown in Fig. 2. In addition, the warm bias in the north-west of the ablation zone is enhanced by the surface albedo feedback as a consequence of the overestimation of the bare ice exposure. However, it should be noted that these temperature biases are statistically not significant.

As conclusion, the negative SMB anomaly in the north-west of the ice sheet is compensated by the overestimation of the SMB in the south of the ice sheet if MAR is forced by CanESM2 in respect to the ERA-40 forced simulation. This explains why the SMB simulated by MAR forced by CanESM2 and by ERA-40 compare very well at the scale of the whole Greenland ice sheet.

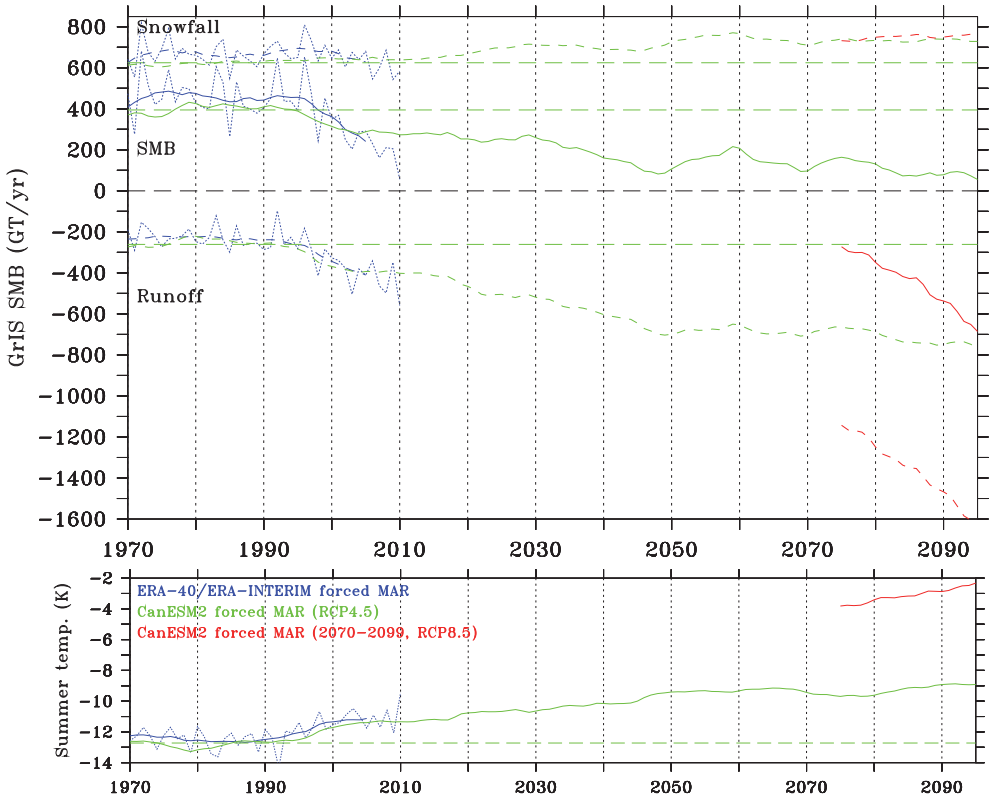

Fig. 5. Time series of the annual Greenland ice sheet snowfall , run-off SMB (top in GT/yr) and summer temperature (below in °C) simulated by MAR forced by ERA-40 over 1970–1999 (in blue), by ERA-INTERIM over 2000-2010 (in blue) and by the CanESM2 based Historical experiment over 1970-2005 (in green), by the RCP4.5 experiment over 2006-2099 (in green) and by the RCP8.5 experiment over 2070-2099 (in red). A 10 year running mean is applied here. Finally, the annual values of the ERA-40/ERA-INTERIM forced simulation (in dotted red) as well as the 1970–1999 average of the CanESM2 forced simulation (in dashed blue) are also shown

5. SMB future projection from CanESM2 forced MAR

5.1 Trends of the SMB components

In respect to the 1970–1999 period simulated by MAR forced by CanESM2, MAR projects for 2070–2099 a decreasing of the SMB of $\sim +75\%$ (resp. $\sim +215\%$) if it is forced by the CanESM2 RCP 4.5 (resp. RCP 8.5) experiment (see Table 4 and Fig. 5). For both scenarios, MAR projects a precipitation increase ($\sim +25\%$ for RCP 4.5 and $\sim +40\%$ for RCP 8.5) that is not large enough to compensate the run-off increase ($\sim +175\%$ for RCP 4.5 and $\sim +420\%$ for RCP 8.5) according to IPCC (2007). The snowfall increase should occur mainly in winter. In summer, the precipitation increased concerns only the rainfall because a part of the solid precipitation should fall in liquid phase due to the rising temperature. This one enhances the melt, knowing that rainfall moistens the snowpack which decreases the surface albedo.

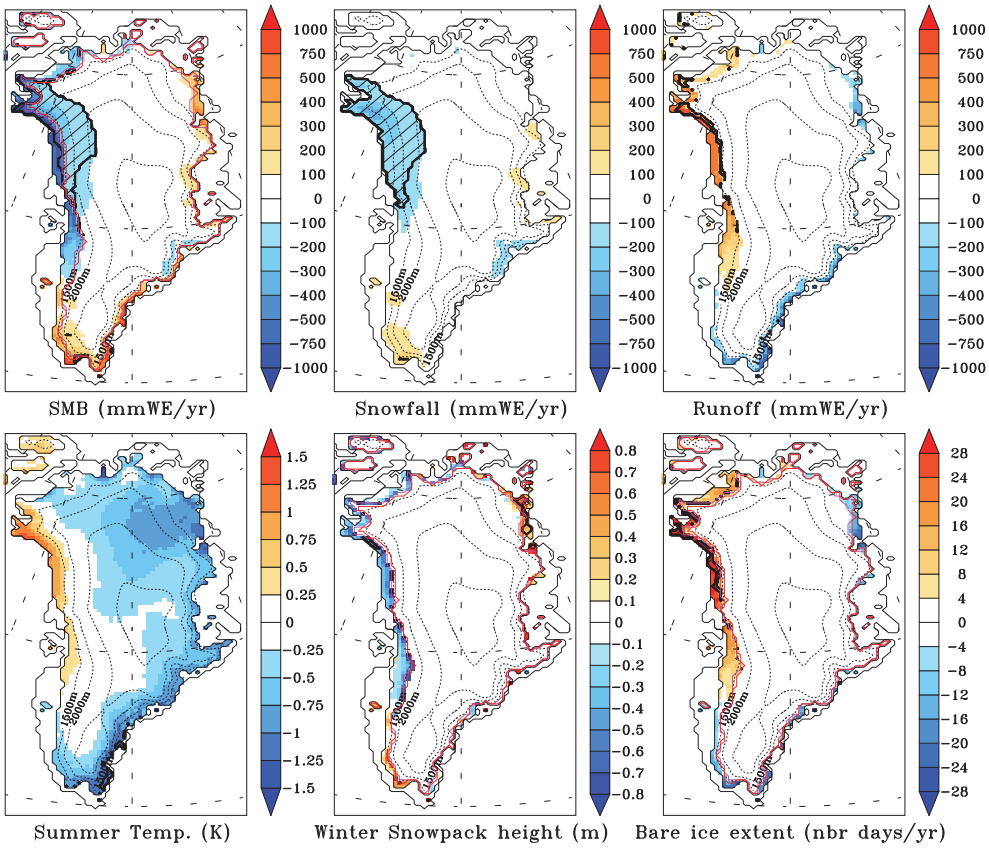

Fig. 6. Difference between the mean 1970–1999 SMB (in mm Water Equivalent/yr), snowfall (in mmWE/yr), run-off (in mmWE/yr), summer near surface temperature (in °C), winter snowpack height (in meter) above bare ice the first of May (.i.e. at the beginning of the summer) and bare ice extent (in number of days where bare ice appears at the surface per year) simulated by MAR forced by CanESM2 and forced by ERA-40. Significant anomalies (those at least twice the magnitude of the 1970–1999 standard deviation) are hatched and bounded by bold black lines. Finally, the mean equilibrium line altitude (i.e. the altitude where the SMB is null) from MAR forced by ERA-40 and forced by CanESM2 is shown respectively in mauve and in red. This altitude line delimits the ablation zone (where the SMB is negative in average) to the accumulation zone (where the SMB is positive).

Scenario	SMB	WSF	SSF	RF	RU	ME	SU	Temperature
RCP 4.5	−294±128	+86±35	+ 20±36	+ 53±10	+458±97	+558±123	−5±2	+3.9±0.8°C
RCP 8.5	−839±245	+277±58	−148±26	+120±35	+1101±271	+1285±302	−14±5	+9.1±0.9°C

Table 4. Anomaly of the annual mean 2070–2099 SMB components simulated by MAR forced by the CanESM2 based RCP 4.5 experiment and RCP 8.5 experiment in respect to the Historical experiment over 1970–1999 (in Gt/yr). The acronyms are described in Table 3. Finally, the annual mean temperature anomalies are also given in °C

The ERA-40/ERA-INTERIM forced time series (Fig 5) shows notably the record low SMB rate simulated by MAR in 2010 and confirmed by the observations (Mernild et al., 2011; Tedesco et al., 2011). The very low SMB rates simulated these last years (2007, 2010) with ERA-INTERIM as forcing should be common at the end of this century with the RCP 4.5 experiment. These observed rates were a combination of lower snowfall and higher run-off than normal. At the end of this century, the run-off and temperature should be higher than those observed the last year but the heavier snowfall in winter should compensate a part of the increase of melt in summer. For RCP 8.5 experiment, MAR simulates never observed negative SMB rates since 50 years (Fettweis et al., 2011a). The snowfall changes are similar to the ones projected for RCP 4.5 but the run-off increase is twice larger than the one projected for RCP 4.5. Finally, the SMB decrease is quasi interrupted in 2050 for RCP 4.5 while the SMB is still decreasing in 2100 with RCP 8.5.
In average, over 2070–2099, the main melt season should still occur between May and September for both scenarios but the melt extent should reach Mid-July 33% of the Greenland ice sheet area for RCP 4.5 (resp. 50% for RCP 8.5) compared to 15% for the current climate (Fig. 4), while the bare ice extent should reach respectively 16% and 22% of the ice sheet area compared to 6% for the present-day climate.

5.2 Spatial changes

In respect to the current climate simulated by MAR forced by CanESM2, MAR projects that for 2070–2099 (RCP 4.5 scenario), SMB should significantly decrease along the ice sheet margin in response to a significant run-off increase resulting from rising summer temperature and that it should slightly increase in the interior of the ice sheet due to heavier snowfall (Fig. 7). The warming is enhanced in the north of the ice sheet because of the decrease of sea ice concentration in the closest parts of the Arctic Ocean according to Franco et al. (2011). In the south of the ice sheet, while the total precipitation is increasing, a part of snowfall becomes rainfall, which enhances the melt. Finally, the bare ice should be exposed in the ablation zone (delimited by the equilibrium line altitude) one month longer by comparison with the current climate. The patterns of changes over 2070–2099 from the RCP 8.5 scenario (not shown here) are similar than those ones from the RCP 4.5 scenario but in more extreme.

6. Future sea level rise projection from SMB changes

According to Fettweis et al. (2008), projected SMB anomalies can be estimated from mean June-July-August (JJA) temperature (T) and annual snowfall (SF) anomalies computed by CanESM2 on the Greenland area by this multiple regression:

$$\Delta SMB \simeq a\frac{T_{RCPxx} - \overline{T_{\text{Historical}}}}{stdev(T_{\text{Historical}})} + b\frac{SF_{RCPxx} - \overline{SF_{\text{Historical}}}}{stdev(SF_{\text{Historical}})} \quad (1)$$

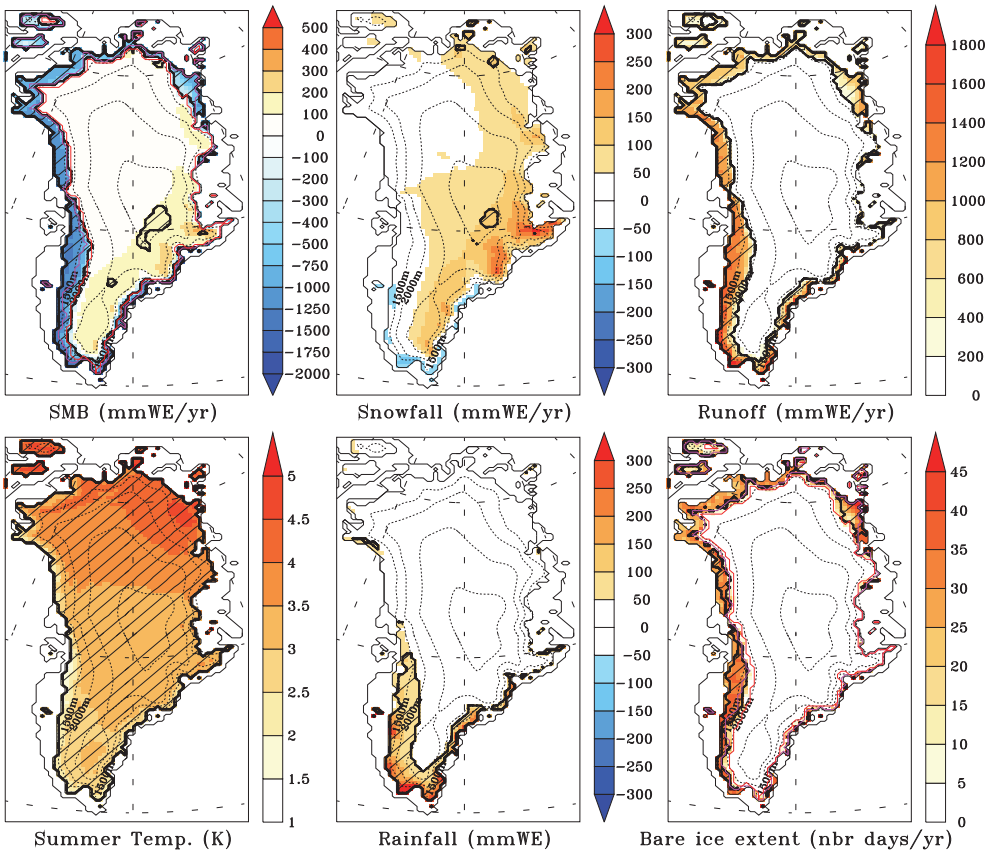

Fig. 7. Difference between the mean 2070–2099 (RCP 4.5 experiment) and the mean 1970-1999 (Historical experiment) SMB (in mm Water Equivalent/yr), snowfall (in mmWE/yr), run-off (in mmWE/yr), summer near surface temperature (in °C), rainfall (in mmWE/yr) and bare ice extent (in number of days where bare ice appears at the surface per year) simulated by MAR forced by CanESM2. Significant anomalies (those at least twice the magnitude of the 1970–1999 standard deviation) are hatched and bounded by bold black lines. Finally, the mean equilibrium line altitude from MAR forced by CanESM2 over 1970–1999 (Historical scenario) and forced by CanESM2 over 2070–2099 (RCP 4.5 scenario) are shown in mauve and in red respectively.

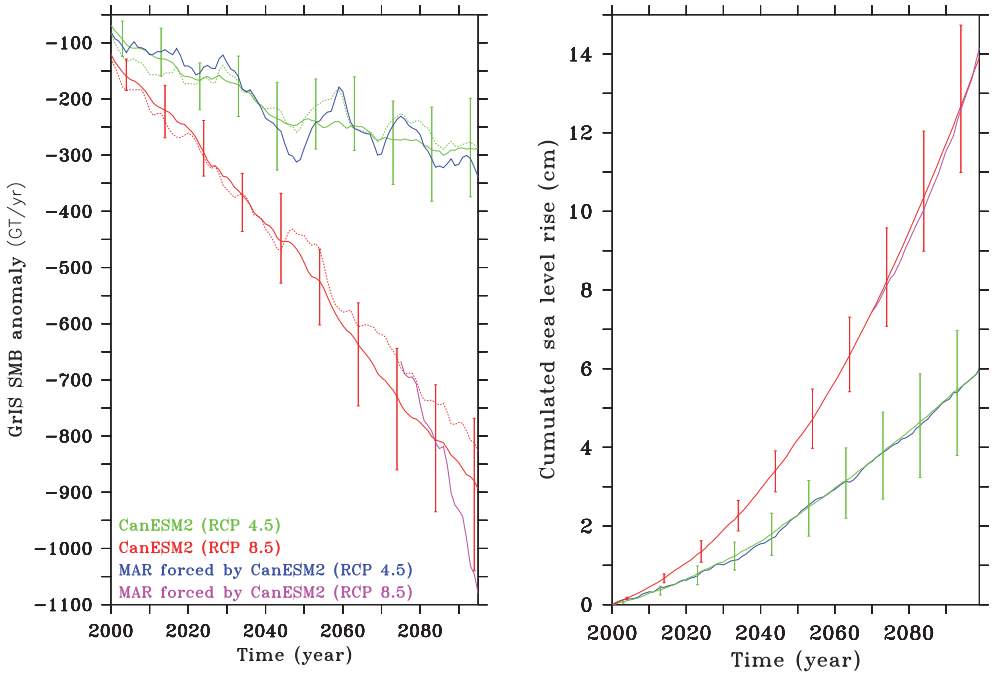

Fig. 8. Left) Future projection of anomalies of the Greenland ice sheet SMB simulated by MAR and retrieved from CanESM2 temperature and precipitation anomalies for the RCP 4.5 and RCP 8.5 scenarios in respect to the 1970–1999 period. For the CanESM2 based time series, the average over all the five available runs is plotted in solid line and the error bar gives the range around this average. The run (called *r1i1p1*) of CanESM2 used for forcing MAR is plotted in dotted line. Finally, a 10-year running mean is applied here and units are GT/yr. Right) The corresponding cumulated sea level rise from SMB changes is shown in cm. The computations use an ocean area of 361 million km^2.

where a and b are two constant parameters, T_{RCPxx} (resp. SF_{RCPxx}) is the JJA temperature (resp. the annual snowfall) from the CanESM2 outputs for the RCP 4.5 or the RCP 8.5 scenario, $\overline{T_{\text{Historical}}}$ is the mean JJA temperature over 1970–1999 from the CanESM2 outputs for the Historical experiment and $stdev(T_{\text{Historical}})$ is the standard deviation around this average. The values of the parameters a and b can be found for a fixed value of the ratio $k = a/b$ by imposing that the standard deviation of the SMB estimated by the CanESM2 temperature and precipitation time series from the Historical experiment (1970–1999) is 106 km^3 yr^{-1} as simulated by MAR forced by ERA-40 over this period. Further details and caveats about the multiple regression model and the parameters it uses are given in Fettweis et al. (2008). The values of $k = a/b$ used here (-1.25 for RCP 4.5 and -5.0 for RCP 8.5) are chosen in order to have the best comparison between the projected sea level rise time series simulated by MAR and the one retrieved from the CanESM2 outputs as shown in Fig. 8. Different values of k are needed for both RCP 4.5 and RCP 8.5 scenarios i.e. the weight of the temperature variability against the precipitation variability in the SMB variability is not the same. For RCP 4.5, the

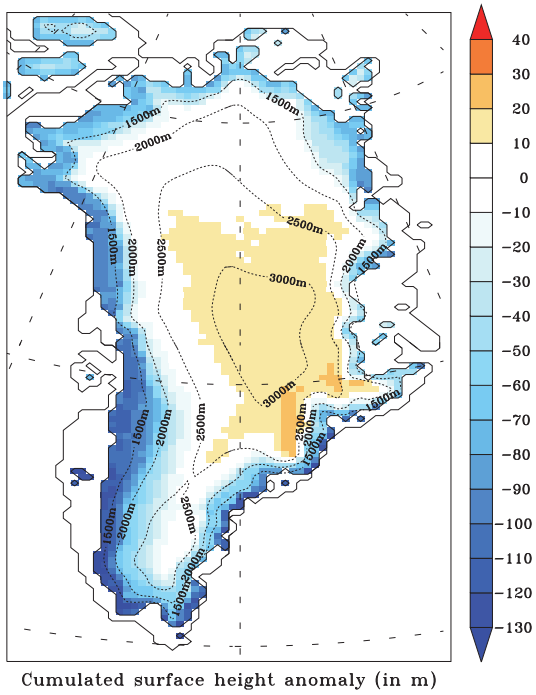

Fig. 9. Cumulated surface height anomaly (in meters) from 2000 to 2100 simulated by MAR for the RCP 4.5 scenario. The anomalies are computed in respect to the 1970–1999 period.

10-year running means of MAR and CanESM2 SMB projections compare well and the value of k used is in agreement with Fettweis et al. (2008). It is not the case for RCP 8.5. This means that the response of SMB to extreme rising temperature as projected by RCP 8.5 seems to be not a linear function of the temperature anomalies as assumed in Eq. 1 but rather a quadratic or exponential function due to the positives feedbacks (e.g. the albedo) which accelerate the surface melt. However, future projections of SMB simulated by MAR forced by RCP 8.5 over 2006-2069 are needed to confirm this hypothesis.

Although the large uncertainties in Eq. 1 resulting from the choice of a fixed value for $k = a/b$ and the hypothesis of linearity in the temperature dependence, the 10-year running means of MAR and CanESM2 SMB projections give the same sea level rise at the end of this century (see Fig. 8). The use of Eq. 1 with the four other runs from CanESM2 (in addition to the run used to force MAR) allows to estimate uncertainties coming from the forcing in our future projections. In 2100, we project a sea level rise coming from changes in Greenland ice sheet SMB estimated to be $\sim +6.5 \pm 1.5$ cm and $\sim +14 \pm 2$ cm for the CanESM2 based RCP 4.5 and RCP 8.5 experiment respectively. The projections for the RCP 4.5 scenario ($+4^{\circ}$C in 2070–2099 compared to 1970–1999) are in full agreement with the projections made for the SRES A1B scenario by Franco et al. (2011) while the projections for the RCP 8.5 scenario are out of range from previous studies (IPCC, 2007) because the warming projected by RCP 8.5 scenario ($+9^{\circ}$C) is larger than the most pessimistic scenario used in the IPCC AR4.

In addition to the uncertainties linked to the models/scenarios, it should be noted that these projections do not take into account changes in ice dynamics and surface topography as

described in Gregory and Huybrechts (2006). Only changes in SMB are considered here and the topography of the Greenland ice sheet is fixed during the simulation although successive annual negative Greenland ice sheet mass rates induce a decrease of the surface height in the ablation zone as shown in Fig. 9 and so, a warming and an acceleration of the melt. For the RCP 4.5 scenario, the cumulated surface height anomalies could be higher than 100 m in 2100 inducing a warming of about 1°C for these pixels in dry atmospheric conditions.

7. Conclusion

Future projections of the Greenland ice sheet SMB were carried out over 2006–2100 for the scenarios RCP 4.5 and RCP 8.5 with the regional climate model MAR forced by the global model CanESM2. The CanESM2 model has been chosen because it is one of the global models from the CMIP5 data base which simulates the best the current climate at 500hPa over Greenland in respect to the European reanalysis. The differences between MAR forced by the ERA-40 reanalysis and forced by CanESM2 over 1970–1999 are not statistically significant except in the north-west of the ice sheet. However, at the scale of the whole Greenland ice sheet, MAR forced by ERA-40 and CanESM2 over current climate compare very well.

As future projections, MAR simulates a significant decrease of the SMB along the ice sheet margin due to increasing melt and a low SMB increase in the interior of the ice sheet due to heavier snowfall. At the scale of the ice sheet, the increase of precipitation does not compensate the increase of melt and MAR simulates a mean surface mass loss of about ~ -300 (resp. ~ -800) GT/yr over 2070–2099 for the RCP 4.5 (resp. RCP 8.5) scenario in respect to current climate (1970–1999). These surface mass losses correspond to cumulated sea level rises of about $\sim +6.5 \pm 1.5$ and $\sim +14 \pm 2$ cm in 2100 respectively. The error ranges in these projections estimate the uncertainties coming from CanESM2 used to force these regional projections. The uncertainties coming from MAR are difficult to evaluate in view of lack of in situ data of SMB at the scale of the whole Greenland ice sheet. Knowing that the future projections of CanESM2 are in the range of other global models of the CMIP5 multi-model data base and that the SMB simulated by MAR compare well with rates coming from other regional models (Fettweis, 2007), this shows that the biggest uncertainties for sea level rise come rather from the used scenario than from the models themselves. However, future projections of MAR forced by another global model (e.g. HadGEM2-ES) from the CMIP5 data base will allow to evaluate better the uncertainties coming from the forcing model.

It is important to note that these projections of sea level rise from Greenland ice sheet mass loss do not take into account changes in ice dynamics (influencing the mass changes from iceberg calving) and in surface topography which could amplify the deglaciation of Greenland due to the positive elevation feedback. At the end of this century, according to the RCP 4.5 scenario, cumulated anomalies of surface height could reach 150m in some areas along the ice sheet margin, emphasizing the necessity of taking into account changes in topography. That is why it will be very interesting to couple MAR with an ice sheet model in addition to the coupling with a snow model to evaluate the feedbacks due to elevation and ice mask changes to the SMB. Moreover, this double coupling will allow to evaluate changes in total Greenland ice sheet mass balance and so to evaluate the sea level rise coming from all changes of mass of the ice sheet.

8. Acknowledgment

Xavier Fettweis is a postdoctoral researcher of the Belgian National Fund for Scientific Research. For their roles in producing, coordinating, and making available the CMIP5 model output, we acknowledge the climate modelling groups (listed in Table 1 of this paper), the World Climate Research Programme's (WCRP) Working Group on Coupled Modelling (WGCM), and the Global Organization for Earth System Science Portals (GO-ESSP). Finally, this work was partly supported by funding from the ice2sea programme from the European Union 7th Framework Programme, grant number 226375 (ice2sea contribution number 046).

9. References

Bamber, J.L., R.L. Layberry, S.P. Gogenini (2001): A new ice thickness and bed data set for the Greenland ice sheet 1: Measurement, data reduction, and errors, Journal of Geophysical Research, 106 (D24): 33773-33780.

Brun, E., David, P., Sudul, M., and Brunot, G.: A numerical model to simulate snowcover stratigraphy for operational avalanche forecasting (1992), J. Glaciol., 38, 13–22.

Box, J. E., Bromwich, D. H., and Bai, L.-S. (2004): Greenland ice sheet surface mass balance for 1991–2000: application of Polar MM5 mesoscale model and in-situ data, J. Geophys. Res., 109(D16), D16105, doi:10.1029/2003JD004451.

Gallée, H. and Schayes, G. (1994): Development of a three-dimensional meso-γ primitive equations model, Mon. Wea. Rev., 122, 671–685.

Gallée, H., Guyomarc'h, G. and Brun, E. (2001): Impact of the snow drift on the Antarctic ice sheet surface mass balance: possible sensitivity to snow-surface properties, Boundary-Layer Meteorol., 99, 1–19.

Gregory, J. and Huybrechts, P. (2006): Ice-sheet contributions to future sea-level change, Philos. T. R. Soc. A, 364, 1709–1731.

Fettweis, X., Gallée, H., Lefebre, L., and van Ypersele, J.-P. (2005): Greenland surface mass balance simulated by a regional climate model and comparison with satellite derived data in 1990–1991, Clim. Dyn., 24, 623–640, doi:10.1007/s00382-005-0010-y.

Fettweis, X. (2007): Reconstruction of the 1979–2006 Greenland ice sheet surface mass balance using the regional climate model MAR, The Cryosphere, 1, 21-40, doi:10.5194/tc-1-21-2007.

Fettweis X., Hanna E., Gallé H., Huybrechts P., Erpicum M. (2008): Estimation of the Greenland ice sheet surface mass balance for the 20th and 21st centuries, The Cryosphere, 2, 117-129.

Fettweis X., Mabille G., Erpicum M., Nicolay, S., and van den Broeke M. (2011a): The 1958–2009 Greenland ice sheet surface melt and the mid-tropospheric atmospheric circulation, Clim. Dynam., Vol. 36 (1-2), 139-159, doi:10.1007/s00382-010-0772-8.

Fettweis, X., Tedesco, M., van den Broeke, M., and Ettema, J. (2011b): Melting trends over the Greenland ice sheet (1958–2009) from spaceborne microwave data and regional climate models, The Cryosphere, 5, 359-375, doi:10.5194/tc-5-359-2011.

Franco B., Fettweis X., Erpicum, M. and Nicolay S.(2011): Present and future climates of the Greenland ice sheet according to the IPCC AR4 models, Clim. Dynam., Vol. 36 (9), 1897-1918, doi:10.1007/s00382-010-0779-1.

IPCC, 2007: Climate Change 2007: The Physical Science Basis. Contribution of Working Group I to the Fourth Assessment Report of the Intergovernmental Panel on Climate Change [Solomon, S., D. Qin, M. Manning, Z. Chen, M. Marquis, K.B. Averyt, M.Tignor and

H.L. Miller (eds.)]. Cambridge University Press, Cambridge, United Kingdom and New York, NY, USA.

Lefebre, F., Gallée, H., van Ypersele, J., and Greuell, W. (2003): Modeling of snow and ice melt at ETH-camp (west Greenland): a study of surface albedo, J. Geophys. Res., 108(D8), 4231, doi:10.1029/2001JD001160.

Lefebre, F., Fettweis, X., Gallée, H., van Ypersele, J., Marbaix, P., Greuell, W., and Calanca, P. (2005): Evaluation of a high-resolution regional climate simulation over Greenland, Clim. Dyn., 25, 99–116, doi:10.1007/s00382-005-0005-8.

Mernild, S.H., Liston, G.E., and Hasholt, B. (2008): East Greenland freshwater run-off to the Greenland-Iceland-Norwegian Seas 1999-2004 and 2071-2100, Hydrological Processes, 22(23), 4571–4586.

Mernild, Sebastian H., Glen E. Liston, Christopher A. Hiemstra, Jens H. Christensen, (2010): Greenland Ice Sheet Surface Mass-Balance Modeling in a 131-Yr Perspective, 1950–2080. J. Hydrometeor, 11, 3–25, doi: 10.1175/2009JHM1140.1.

Mernild, S. H., Knudsen, N. T., Lipscomb, W. H., Yde, J. C., Malmros, J. K., Hasholt, B., and Jakobsen, B. H. (2011): Increasing mass loss from Greenland's Mittivakkat Gletscher, The Cryosphere, 5, 341-348, doi:10.5194/tc-5-341-2011.

Moss, R.H., Edmonds, J.A., Hibbard, K., Manning, M., Rose, S.K., van Vuuren, D.P., Carter, T.R., Emori, S., Kainuma, M., Kram, T., Meehl, G., Mitchell, J., Nakicenovic, N., Riahi, K., Smith, S., Stouffer, R.J., Thomson, A., Weyant, J. and Wilbanks, T. (2010): The next generation of scenarios for climate change research and assessment. Nature, doi:10.1038/nature08823.

Nick, F. M., Vieli, A., Howat, I. M. and Joughin, I (2009). Large-scale changes in Greenland outlet glacier dynamics triggered at the terminus. Nature Geoscience 2, 110-114, doi:10.1038/ngeo394.

Sundal AV, Shepherd A, Nienow P, Hanna E, Palmer S, Huybrechts P. (2011) Melt-induced speed-up of Greenland ice sheet offset by efficient subglacial drainage, Nature, 469(7331), 521–524, doi:10.1038/nature09740.

Tedesco, M., Fettweis, X., van den Broeke, M., van de Wal, R., Smeets, P., van de Berg, W. J., Serreze, M., and Box, J. (2011). The role of albedo and accumulation in the 2010 melting record in Greenland. Environmental Research Letters, 6(1).

Van den Broeke, M. R., Bamber, J., Ettema, J., Rignot, E., Schrama, E., van de Berg, W. J., van Meijgaard, E., Velicogna, I., and Wouters, B. (2009): Partitioning recent Greenland mass loss, Science, 326, 984–986.

Zwally, J. H., Abdalati, W., Herring, T., Larson, K., Saba, J., and Steffen, K. (2002): Surface Melt-Induced Acceleration of Greenland Ice-Sheet Flow, Science, 297, 218–222.